Enhanced Phosphorus Locking by Novel Lanthanum/Aluminum-Hydroxide Composite: Implication for Eutrophication Control

Rui Xu[†, ‡], Meiyi Zhang[†], Robert J.G. Mortimer[§], and Gang Pan[*, †, §]

[†] Research Center for Eco-Environmental Sciences, Chinese Academy of Sciences, Beijing 100085, China

[‡] University of Chinese Academy of Sciences, Beijing 100049, China

[§] School of Animal, Rural and Environmental Sciences, Nottingham Trent University, Brackenhurst Campus, NG25 0QF, UK

* Corresponding author: gpan@rcees.ac.cn (GP)

Abstract: Lanthanum (La) bearing materials have been widely used to remove phosphorus (P) in water treatment. However, it remains a challenge to enhance phosphate (PO_4) adsorption capacity and La usage efficiency. In this study, La was co-precipitated with aluminum (Al) to obtain a La/Al-hydroxide composite (LAH) for P adsorption. The maximum PO_4 adsorption capacities of LAH (5.3% La) were 76.3 and 45.3 mg P g^{-1} at pH 4.0 and 8.5, which were 8.5 and 5.3 times higher than those of commercially available La-modified bentonite (Phoslock®, 5.6% La), respectively. P K-edge X-ray absorption near edge structure analysis showed that PO_4 was preferentially bonded with Al under weakly acid conditions (pH 4.0), while tended to associate with La under alkaline conditions (pH 8.5). La L_{III}-edge extended X-ray absorption fine structure analysis indicated that PO_4 was bonded on La sites by forming inner sphere bidentate-binuclear complexes and oxygen defects exhibited on LAH surfaces, which could be active adsorption sites for PO_4. The electrostatic interaction, ligand exchange and oxygen defects on LAH surfaces jointly facilitated PO_4 adsorption but with varied contribution under different pH conditions. The combined contribution of two-component of La and Al may be an important direction for the next generation of commercial products for eutrophication mitigation.

TOC

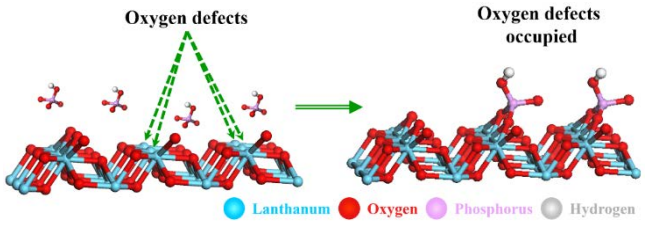

Introduction

Excessive phosphorus (P) discharge can trigger severe eutrophication in aquatic environments,[1-3] which may further lead to harmful algal blooms, deterioration of water quality, and eventually, ecosystem collapse.[4, 5] Over recent decades, various materials have been used for P removal in water bodies.[2] In particular, La-modified materials or La-bearing compounds are often considered as effective geo-engineering tools to lock P from aquatic ecosystems.[6, 7] For instance, the commercial product Phoslock®, a La-modified bentonite clay, has been used for internal P loads control in 200 water bodies.[2, 8]

Previous studies suggest that the binding ability between La and PO_4 anions dominates P locking by La-bearing materials.[9-11] Ligand exchange is generally considered as the main mechanism of PO_4 affinity to La-bearing materials.[9, 10] It is well known that the ability of ligand exchange depends on the surface charge of the adsorbent.[12] However, existing La-modified materials (including Phoslock®) often have a negative surface charge in natural waters,[10, 13] which is not favorable for attracting $H_2PO_4^-$ or HPO_4^{2-} from the viewpoint of electrostatic interaction. If the surface charge of La-modified material could be made positive, it would attract more PO_4 anions.[12] We hypothesize that synthesizing a La-bearing adsorbent with positive surface charge would enable a two component mechanism involving both electrostatic interaction and ligand exchange to improve PO_4 adsorption capacity and La use efficiency. This requires a new host material for La in order to develop a more efficient PO_4 adsorbent.

Aluminum (Al) compounds are also widely used for P removal in water treatment.[14] Al (hydro)oxide is effective at adsorbing P selectively in the presence of competing anions such as Cl^-, NO_3^-, HCO_3^- and SO_4^{2-}.[15] It is also abundant in nature, low cost and has a high point of zero charge (pH_{PZC}).[14] Al compounds could potentially be a host

material for La in synthesizing a new adsorbent with positive surface charge. On the other hand, it has been reported that the effectiveness of Al treatment depends on the pH in waters,[16] because Al compounds are prone to desorption of PO_4 under alkaline conditions.[17, 18] Moreover, the ecological effect of aluminum has become a concern in aquatic research.[17, 19] Owing to the high affinity between La and PO_4 anions, if an Al compound is incorporated in the fabrication with La, the PO_4 adsorbed by La/Al composite may be more stable over a wide pH range, which is important for practical remediation engineering under field conditions.

As an element-specific and in situ method to detect the molecular structures of reacting species, X-ray absorption fine structure (XAFS) spectroscopy, including X-ray absorption near edge structure (XANES) and extended X-ray absorption fine structure (EXAFS) spectroscopy, has been developed for determining the properties of PO_4 bonding on solid surfaces.[11, 20, 21] P K-edge XANES has been used to study PO_4 adsorption in single or binary systems of Fe/Al-hydroxide materials, which can distinguish PO_4 contents associated with Fe- or Al- hydroxide.[20, 22, 23] EXAFS could provide additional insights for PO_4 bonding mode by detecting the local structure of metal elements reacted with PO_4.[11] By using La L_{III}-edge EXAFS spectroscopy, the PO_4 bonded on Phoslock® was proved to be an insoluble rhabdophane ($LaPO_4 \cdot nH_2O$, $n \leq 3$).[11] However, to the best of our knowledge, little information is available about the effect of La local structure on PO_4 adsorption capacity and its transformation after reaction with PO_4.

Here, a La/Al-hydroxide composite (LAH) with high PO_4 adsorption efficiency was synthesized by a co-precipitation method. Three LAH composites with different La:Al molar ratios of 1:30, 1:20 and 1:10 were prepared in order to investigate the role of La in LAH for PO_4 adsorption. Batch experiments were conducted to determine the

adsorption and desorption properties of PO_4 on LAH. P K-edge XANES spectroscopy was used to investigate the proportions of PO_4 associated with Al relative to La. La L_{III}-edge EXAFS spectroscopy was used to detect the local atomic structure changes around the La (III) ion before and after PO_4 adsorption to elucidate the adsorption mechanism of PO_4 on LAH surfaces. The objective of this study is to synthesize a highly efficient PO_4 adsorption material and to investigate its mechanism at the molecular level, so that the methodology could be used to guide new development of geo-engineering materials for eutrophication management.

Materials and methods

LAH synthesis and characterization. Predetermined amounts of analytical grade $LaCl_3 \cdot 7H_2O$ and $AlCl_3$ were dissolved into 200 mL deionized water to obtain La/Al molar ratios of 1:30, 1:20 and 1:10 (LAH-1/30, LAH-1/20 and LAH-1/10). Under stirring, 2 mol L^{-1} NaOH aqueous solution was added dropwise to the mixed solutions at 333 K until pH 9.0. Then the mixture was stirred for 2 h and aged for 24 h at 333 K. Precipitates were washed three times with deionized water and freeze-dried for 24 h. Powders of $Al(OH)_3$ and $La(OH)_3$ were synthesized by the same process to act as controls (Details are provided in the Supporting Information).

To obtain the exact content of La and Al in the LAH, samples were digested in 6 mol L^{-1} HCl and the chemistry of the resultant solutions was determined using an inductively coupled plasma optical emission spectrometer (ICP-OES, Optima 8300, PerkinElmer, USA). Brunauer-Emmett-Teller (BET) surface areas and pore size distributions were examined by a Micromeritics ASAP 2020 static volumetric analyzer. LAH morphologies were observed using field emission scanning electron microscopy (FESEM, SU 8020, Hitachi, Japan). X-ray powder diffraction (XRD) data of the LAH were recorded on an X'Pert PRO MPD X-ray diffractometer (PANalytical, The

Netherlands) with a Cu-K radiation (λ = 1.5408) at 40 kV and 40 mA in the 2θ range of 5° to 90°. Electron paramagnetic resonance (EPR) spectrum of LAH-1/10 was recorded on a JEOL JES-FA200 EPR spectrometer (Japan) at room temperature. Zeta (ζ) potential analysis of LAH was measured by a Zetasizer Nano ZS potential analyzer (Malvern Instrument Ltd., United Kingdom). Phoslock® (Phoslock® Water Solutions Ltd, Australia) was also characterized by the same procedures described above.

Adsorption and desorption experiments. In order to identify the influence of pH on the equilibrium adsorption capacity, adsorption experiments of PO_4 on LAH were conducted in polypropylene tubes at pH 4.0 ~ 10.0. LAH (1 g L^{-1}) were added to 50 mL polypropylene tubes with initial P concentration 80 mg P L^{-1} in 0.01 mol L^{-1} NaCl background and shaken at 170 rpm at 298 K for 48 h. The solution pH was maintained constant with 0.01 mol L^{-1} HCl and NaOH.

Adsorption isotherm experiments were conducted in 50 mL polypropylene tubes by mixing various concentrations of KH_2PO_4 solutions with 1 g L^{-1} adsorbents in 0.01 mol L^{-1} NaCl background. The mixture was stirred at 298 K for 48 h allowing the adsorption to reach equilibrium. pH 4.0 (pH for maximum PO_4 adsorption in this study, Figure S3) and pH 8.5 (up limit pH for lakes)[24] were chosen to determine the adsorption and desorption behaviors of PO_4. At the end of adsorption isotherm experiments, the exhausted solutions of LAH samples which had initial P concentration 80 mg P L^{-1} were centrifuged to preserve 10 mL suspension at the bottom, and then 0.01 mol L^{-1} NaCl solution was added to keep the same ionic strength. The experimental conditions of desorption experiments were conducted following adsorption studies.

The PO_4 concentration was measured by ascorbic acid method to monitor the absorbance at 880 nm with spectrophotometer (UV-756 PC, Shanghai Sunny Hengping Scientific Instrument CO. LTD, China). The concentrations of released Al^{3+} and La^{3+}

were analyzed by ICP-OES (Optima 8300, PerkinElmer, USA).

XAFS data collection and analysis. Phosphorus K-edge XANES data were collected on Beamline 4B7A at the Beijing Synchrotron Radiation Facility (BSRF), China. The storage ring was operating at 2.5 GeV with current from 250 to 150 mA. A double crystal Si (111) monochromator offered an energy resolution of about 0.6 eV with a beam size of 1.0 × 3.0 mm^2. The incident X-ray energy was calibrated by using the white line of K_2SO_4 (S K-edge) at 2482.4 eV before spectra collection. Spectra were collected in the fluorescence yield (FLY) mode between -30 to +90 eV relative to P K-edge energy at 2152 eV with a minimum step size of 0.3 eV between 2140 and 2180 eV. The P1s peak position of KH_2PO_4 was used to calibrate the P K-edge XANES spectra. La L_{III}-edge EXAFS data were collected on beamline 1W2B at the BSRF, China. The monochromator energy calibration was monitored to 5483 eV using a vanadium foil as an internal standard with a transmission chamber detector. The moist samples were fixed in a Teflon cell and sealed with Mylar film during EXAFS measurement.[25] An average of three scans was performed to achieve suitable single/noise, and no obvious change in spectral data was observed during the three scans. The spectral data were processed following the standard procedures of background absorption removal, normalization, k-space conversion and Fourier transformation. Details for data collection and analysis were given in the Supporting Information.

Results

Characterization. The physiochemical properties of the three synthesized LAH materials, commercial product Phoslock® and $Al(OH)_3$ were summarized in Table 1. The La mass proportion of LAH-1/30 was 5.3%, which was close to that of Phoslock® (5.6%). The La mass proportions of LAH-1/20 and LAH-1/10 were 7.8% and 13.1%,

respectively. The BET surface areas of LAH-1/30, LAH-1/20 and LAH-1/10 were 107.1, 121.0 and 99.3 $m^2 g^{-1}$, respectively, which were much higher than those of Phoslock® (38.2 $m^2 g^{-1}$) and $Al(OH)_3$ (51.2 $m^2 g^{-1}$).

Table 1. General characteristics of LAH, Phoslock® and $Al(OH)_3$

Adsorbent	La (wt %)	Al (wt %)	surface area ($m^2 g^{-1}$)	pore volume ($cm^3 g^{-1}$)
LAH-1/30	5.3	31.7	107.1	0.34
LAH-1/20	7.8	31.4	121.0	0.39
LAH-1/10	13.1	26.5	99.3	0.31
Phoslock®	5.6	7.8	38.2	0.14
$Al(OH)_3$	-	34.6	51.2	0.06

The XRD analysis suggested that LAH were mainly composed of $Al(OH)_3$ (PDF NO. 74-1119) and $La(OH)_3$ (PDF NO. 36-1481) (Figure 1a). The characterization peaks of $La(OH)_3$ were weaker with increasing La contents, indicating that more amorphous $La(OH)_3$ was formed. The EPR spectrum of LAH-1/10 showed a clear signal at g = 2.0509 (Figure 1b) corresponding to oxygen defects on the surfaces.[26, 27] FESEM images showed that the average particle size of LAH composite was about 8-16 μm and thin flakes appeared on LAH surfaces with increasing La contents (Figure S1).

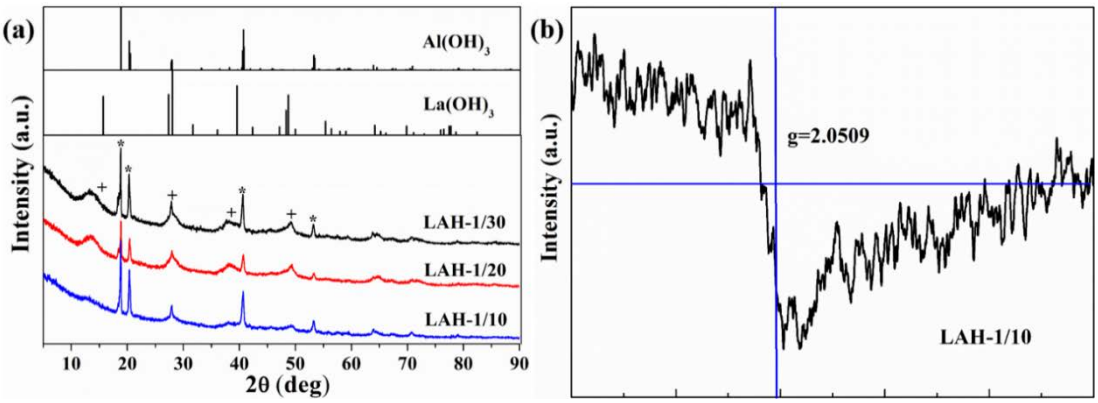

Figure 1. (a) XRD patterns of LAH, in comparison with model compounds of $Al(OH)_3$ and $La(OH)_3$. Asterisks (*), $Al(OH)_3$; Plus (+), $La(OH)_3$. (b) EPR spectrum of LAH-1/10 at room temperature.

The ζ potential of Phoslock® and LAH samples before and after PO_4 adsorption were shown in Figure 2. The LAH had positive surface charge from pH 4.0 to 9.7, while Phoslock® had negative potential from -5.4 to -43.1 mV in the pH range of 4.0 to 10.0. The ζ potential of all LAH materials decreased after PO_4 adsorption at initial P concentration 50 mg P L^{-1}. For LAH-1/30, the ζ potential decreased significantly from about +50 mV (pH 4.0) and +10 mV (pH 8.5) to +11 mV (Figure 2, dot a) and -21 mV (Figure 2, dot b) ($p < 0.001$, paired t-test, SPSS 19.0) after PO_4 adsorption, respectively. The ζ potential of $La(OH)_3$ and $Al(OH)_3$ were also determined, and the pH_{pzc} value of $La(OH)_3$ and $Al(OH)_3$ was approximately 9.4 (Figure S2).

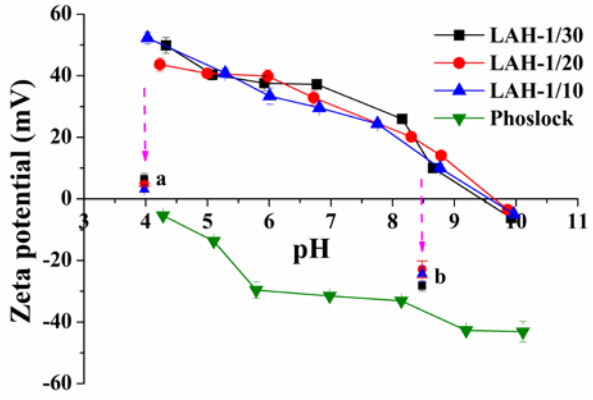

Figure 2. ζ potential of LAH and Phoslock® as a function of pH (solid line), and that of LAH with adsorbed PO_4 at pH 4.0 (dot a) and 8.5 (dot b).

Phosphate adsorption and desorption. The effect of pH on PO_4 adsorption to LAH was investigated in the pH range of 4.0 ~ 10.0 (Figure S3). LAH-1/10 had the highest PO_4 adsorption capacity of 71.6 mg P g^{-1} at pH 4.0 and decreased to 26.1 mg P g^{-1} at pH 10.0. The data showed LAH exhibited a maximum PO_4 adsorption capacity at pH 4.0 and dropped with increasing pH values. Consequently, pH 4.0 (pH for maximum

205 PO_4 adsorption in this study) and pH 8.5 (up limit pH for lakes)[24] were chosen in
206 following experiments to investigate the macro phenomena and micro mechanisms of
207 PO_4 adsorption on LAH.

208 Phosphate adsorption isotherms for LAH were L-curves (Figure 3) and were fitted
209 with the Langmuir model (Table S1). LAH-1/10 had the maximum PO_4 adsorption
210 capacities (Q_m) of 128.2 and 70.4 mg P g^{-1} at pH 4.0 and pH 8.5 (Table S1). The Q_m of
211 LAH-1/30 (5.3% La, Table 1) were 8.5- and 5.3-fold higher than those of Phoslock®
212 (5.6%, Table 1) at pH 4.0 and pH 8.5, respectively. The PO_4 specific adsorptions on
213 Phoslock® and LAH were calculated on the basis of Q_m (Table S1) and BET surface
214 area (Table 1). LAH-1/10 exhibited higher PO_4 specific adsorptions of 1.29 and 0.71
215 mg m^{-2} than those of LAH-1/20 (1.00 and 0.53 mg m^{-2}) and LAH-1/30 (0.71 and 0.42
216 mg m^{-2}) at pH 4.0 and 8.5 (Table S1), respectively. The PO_4 desorption rates of LAH-
217 1/30, LAH-1/20 and LAH-1/10 were 2.54%, 2.01% and 4.05% at pH 4.0, which were
218 reduced to 0.28%, 0.22% and 0.29% at pH 8.5 (Figure S4), respectively.

219 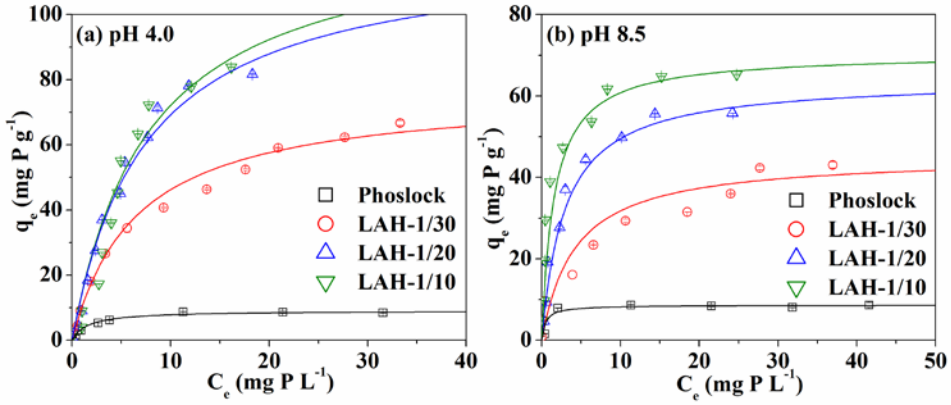

220 **Figure 3.** Langmuir isotherm fitting plots of LAH and Phoslock® at pH 4.0 (a) and pH
221 8.5 (b). The experimental condition: temperature = 298 K, adsorbent dosage = 1 g L^{-1},
222 reaction time = 48 h.

223 In order to assess the ecological risk of LAH to natural water bodies, concentrations
224 of released Al^{3+} and La^{3+} were measured in natural water pH ranges from 7.0 to 9.0

(Figure 4). The maximum concentration of released Al^{3+} was 0.078 mg L^{-1} by LAH-1/30 at pH 9.0 (Figure 4a). LAH-1/10 had the highest released La^{3+} concentration of 0.077 mg L^{-1} at pH 7.0 (Figure 4b). The dissolutions of Al and La from LAH at pH 4.0 to 10.0 were also determined (Figure S5). The maximum Al and La dissolved proportions were 0.58% by LAH-1/30 and 0.55% by LAH-1/10 at pH 4.0, respectively.

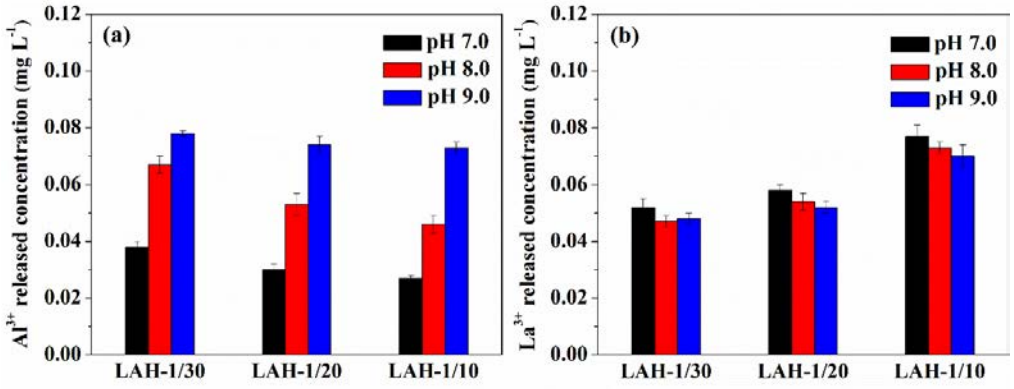

Figure 4. Concentrations of released Al^{3+} and La^{3+} from pH 7.0 to 9.0. The experimental condition: temperature = 298 K, adsorbent dosage = 1 g L^{-1}, reaction time = 48 h.

P K-edge XANES. Normalized P K-edge XANES spectra for LAH-1/30 samples after PO_4 adsorption with initial P concentrations (C_0) 50 and 80 mg P L^{-1} at pH 4.0 and 8.5 were shown in Figure 5. LCF results showed that the proportions of PO_4 bonded with La-hydroxide (La-P) for LAH-1/30 with adsorbed PO_4 at pH 4.0 were 32.6% and 45.0%, which were less than those with Al-hydroxide (Al-P) of 67.4% and 55.0% (Figure 5a, b). However, for LAH-1/30 with adsorbed PO_4 at pH 8.5, the proportions of PO_4 boned with La-hydroxide (La-P, 52.6% and 54.1%) were higher than those with Al-hydroxide (Al-P, 47.4% and 45.9%) (Figure 5c, d).

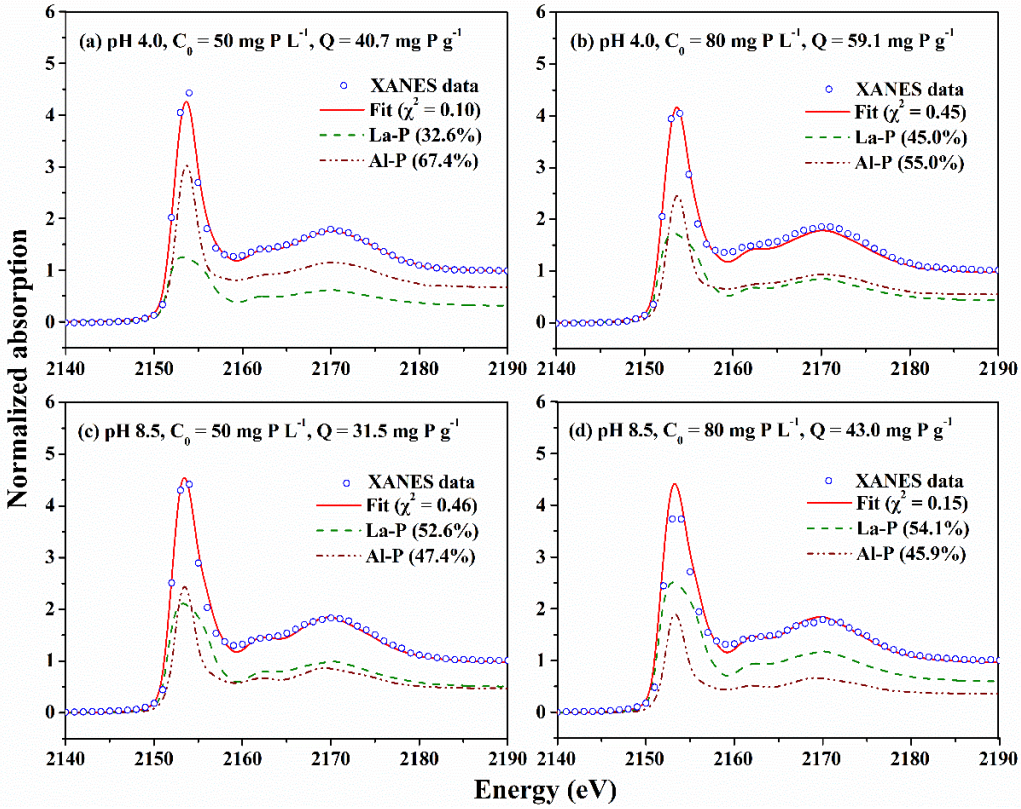

Figure 5. Linear combination fitting for LAH-1/30 samples after PO_4 adsorption with weighted components of La-P and Al-P. The experimental condition: (a) pH 4.0 with C_0 50 mg P L^{-1}, (b) pH 4.0 with C_0 80 mg P L^{-1}, (c) pH 8.5 with C_0 50 mg P L^{-1} and (d) pH 8.5 with C_0 80 mg P L^{-1}.

La L_{III}-edge EXAFS. In order to investigate the La local coordination environment, the La L_{III}-edge EXAFS spectra analysis was conducted (Figure 6). Spectra of commercial $La(OH)_3$ and Phoslock® were also collected (Figure S6, S7). The first shell La-O of LAH was at a distance of 2.55 ~ 2.60 Å (Table S2), which was very close to that of the La-O shell of $La(OH)_3$ (2.5 ~ 2.6 Å).[28] The La-O CN of LAH-1/30, LAH-1/20 and LAH-1/10 were 6.8 ± 0.7, 6.5 ± 0.4 and 6.1 ± 0.3 (Table S2), respectively. Al atoms were detected at 3.10 ~ 3.11 Å with La-Al CN of 2.6 ± 0.9, 2.2 ± 0.5 and 1.4 ± 0.5 to LAH-1/30, LAH-1/20 and LAH-1/10 (Table S2), respectively. The La-O CN of LAH samples after PO_4 adsorption were 7.3 ~ 7.6 (Table S3). A new La-P shell in LAH samples with adsorbed PO_4 was detected at a distance of 3.20 ~ 3.31 Å and the average

CN of La-P shell were about 2.5 (Table S3). Additionally, the original CN of La-O shell in Phoslock® was 8.9 ± 0.8 (Table S2), which was about 8.8 after PO_4 adsorption (Table S3). With increased La loading, the intensity of La-O peak became weaker in LAH composite (Figure S8b). Besides, the attenuation rate of χ(k) of LAH was faster than that of $La(OH)_3$ (Figure S8a). In accordance with XRD spectra (Figure 1a), La L_{III}-edge EXAFS spectra also proved that amorphous $La(OH)_3$ was formed in LAH during the La/Al co-precipitation process.

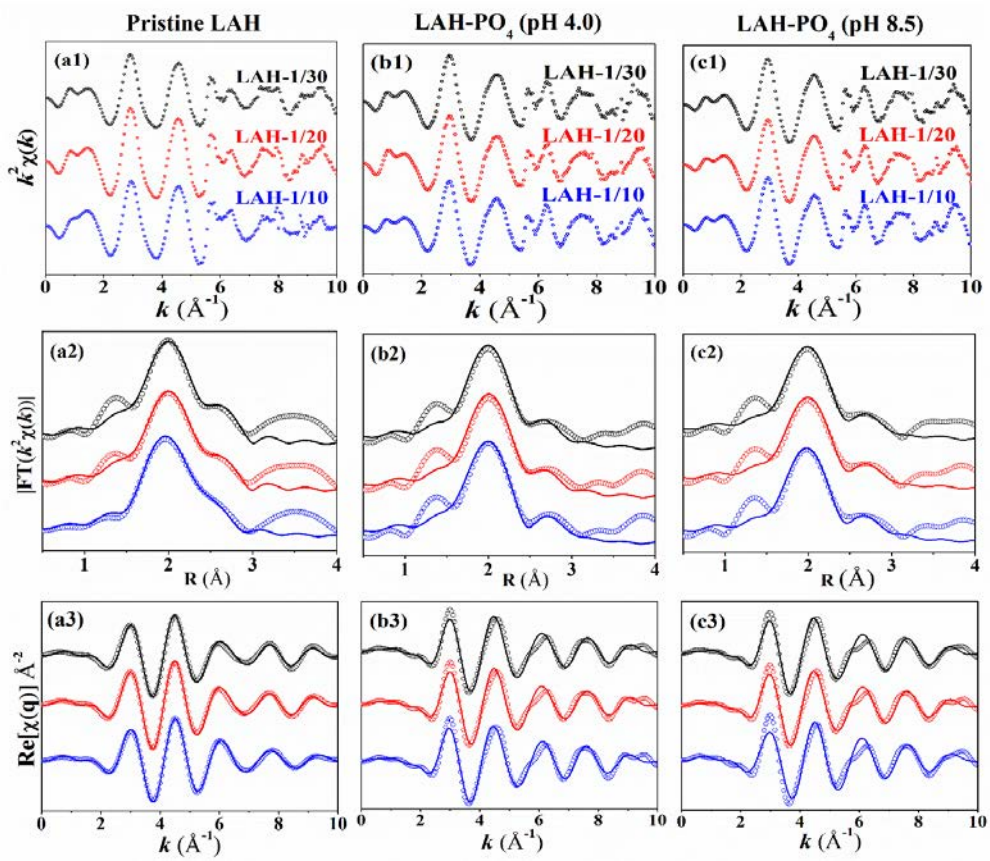

Figure 6. Normalized k^2-weighted La L_{III}-edge EXAFS spectra (a1, b1, c1), the corresponding Fourier transformed magnitude (a2, b2, c2) and real (q) part of Fourier transform (c1, c2, c3) of pristine LAH, LAH with adsorbed PO_4 at pH 4.0 (LAH-PO_4, pH 4.0) and LAH with adsorbed PO_4 at pH 8.5 (LAH-PO_4, pH 8.5). Samples of LAH-1/30 (black), LAH-1/20 (red) and LAH-1/10 (blue). The dotted lines were observed spectra and the solid lines were fitting curves.

Discussion

Electrostatic attraction and ligand exchange. The ζ potential data showed that the pH_{PZC} value of LAH-1/30, LAH-1/20 and LAH-1/10 was approximately 9.7 (Figure 2). When solution pH was lower than 9.7, LAH were protonated and positively charged. Compared to negatively charged Phoslock®, the positively charged surfaces of LAH could attract more negatively charged PO_4 anions by electrostatic interaction over a wide pH range. The results showed that the ζ potential of LAH decreased with increasing pH values (Figure 2). Lower pH is beneficial for the protonation of LAH surfaces, which could enhance the electrostatic attraction between LAH and PO_4 anions. Owing to the higher surface charge and more protonated active sites, LAH-1/30 showed a higher PO_4 adsorption capacity (76.3 mg P g^{-1}, Table S1) at pH 4.0 than that (45.3 mg P g^{-1}, Table S1) at pH 8.5. Although $La(OH)_3$ is also positively charged under natural lake pH conditions (Figure S2),[29] the utility of La (hydro)oxide alone in eutrophication restoration is not recognized as an economic way in view of its high price and relative scarcity. The incorporation of Al hydroxide with La in LAH materials not only maintains high pH_{PZC} values, but also reduces costs compared to using La (hydro)oxide alone.

Changes of solution pH during PO_4 adsorption on LAH-1/30 at initial pH 4.0 and 8.5 were monitored (Figure S9). The solution pH increased from initial pH 4.0 to nearly 6.5 after 24 h and it increased little when initial pH was 8.5 (Figure S9). The increase in pH value was due to the release of OH^- after ligand exchange interaction, indicating that ligand exchange played a primary role in PO_4 adsorption.[9, 10] The surface charges of pristine LAH-1/30 decreased significantly after PO_4 adsorption (Figure 2), suggesting that PO_4 was bonded on LAH surfaces by forming inner-sphere complexes via ligand exchange.[30] In order to demonstrate ligand exchange interaction at the

molecular level, we measured P K-edge XANES spectra of LAH-1/30 samples with adsorbed PO_4 (Figure 5). According to LCF analysis, the proportions of PO_4 bonded with Al-hydroxide were 2.07 and 1.22 times higher than those with La-hydroxide at pH 4.0 (Figure 5a, b). On the contrary, the proportions of PO_4 bonded with Al-hydroxide (Al-P, 47.4% and 45.9%) were less than those with La-hydroxide (La-P, 52.6% and 54.1%) at pH 8.5 (Figure 5c, d). The fitting data showed PO_4 was preferentially bonded with Al in weakly acidic conditions (pH 4.0), while most PO_4 tended to associate with La under alkaline conditions (pH 8.5). The results showed that both La-hydroxide and Al-hydroxide in LAH composite could bind with PO_4 anions by forming inner-sphere complexes.[31, 32] In this study, the XANES measurement provided strong evidence that a ligand exchange mechanism played a role both at pH 4.0 and 8.5.

It was reported that higher alkaline condition (pH 9.5) might result in the dissolution of $Al(OH)_3$ and the release of PO_4 concomitantly.[17] However, the Al^{3+} and PO_4 released proportions in LAH were both very low at alkaline conditions (Figure S4, S5). According to La L_{III}-edge EXAFS analysis, a La-Al shell was formed in LAH samples (Table S2). As the addition of La to alumina could generate new-type Lewis acid site on the surface,[33] the increased La loading in LAH might affect the properties of Al-hydroxide in LAH composite. The Al^{3+} and La^{3+} ions all showed a higher dissolution proportions at lower alkalinity (Figure S5).[34] It has been hypothesized that natural organic matter can impact PO_4 adsorption via the formation of OM-Fe(III)-PO_4 or OM-Al(III)-PO_4 ternary complexes.[35, 36] Hence, we induced that the ternary LAH-Al^{3+}/La^{3+}-PO_4 complex might also be formed when pH changed to the low value of 4.0.

The oxygen defects on La compound. EXAFS analysis showed that La-O CN of LAH-1/30, LAH-1/20 and LAH-1/10 were 6.8 ± 0.7, 6.5 ± 0.4 and 6.1 ± 0.3 (Table S2), respectively. The average La-O CN of LAH composite were approximately 6.5, which

were all less than the saturated La-O CN of 9.0 in $La(OH)_3$.[28] It is generally recognized that lower CN of surface ions may depend on oxygen defects on the surfaces of metal compound.[37-39] Among LAH materials, LAH-1/10 with highest La content (13.1%, Table 1) might had the most amounts of oxygen defects on the surfaces. Additionally, EPR spectrum demonstrated the presence of oxygen defects on the surfaces (Figure 1b). It was reported that the surface defect sites were more reactive than the perfect surfaces.[40, 41] LAH-1/10 with more La loading exhibited higher PO_4 specific adsorptions of 1.29 (pH 4.0) and 0.71 mg m^{-2} (pH 8.5) than those of LAH-1/20 and LAH-1/30 (Table S1), respectively, which might be also attributed to more amounts of oxygen defects on the surfaces. Compared to the mixture of pure $La(OH)_3$ and pure $Al(OH)_3$ to a La/Al molar ratio 1:30, the PO_4 specific adsorption on LAH-1/30 at pH 8.5 (0.42 mg m^{-2}, Table S1) was 1.6 times higher than the mixture (0.26 mg m^{-2}, Figure S10), further supporting that the oxygen defects on LAH surfaces provided special adsorption towards PO_4 anions. The La-O CN of Phoslock® with PO_4 bonded was 8.8 (Table S3), which was similar to its original CN of 8.9 (Table S2). While, the average La-O CN of LAH after PO_4 adsorption increased to 7.5 (Table S3) compared to its original average value of 6.5 (Table S2). The change of La-O in LAH before and after PO_4 adsorption proved the role of oxygen defects on LAH to facilitate PO_4 adsorption. It was reported that the oxygen defects on Al compound were not observed until the material was calcined at above 473 K.[42] Therefore, the role of oxygen defects on La compound for PO_4 adsorption, not Al compound, was the major consideration in present study since the prepared temperature of LAH was 333 K.

After PO_4 adsorption, a new La-P shell was detected in LAH samples (Table S3). The distance of La-P shell was at 3.20 ~ 3.31 Å (Table S3), which was shorter than that of $LaPO_4 \cdot 1.4H_2O$ (3.52 Å) and $LaPO_4$ (4.16 Å).[11] With the bond distance and the

346 average CN (~ 2.5, Table S3) of La-P shell, the PO_4 surface configuration was in
347 agreement with previous EXAFS studies of PO_4 adsorption on goethite/water
348 interface.[43] Hence, the most likely configuration of PO_4 on La site was a bidentate-
349 binuclear complex.[43] The La-PO_4 bonding was a direct evidence to demonstrate the
350 formation of inner-sphere complex of P on La site.

351 **Toxicity analysis.** The release of metal ions is a major concern when using lake
352 restoration materials, which may induce potentially environmental risk and limit their
353 usage as P removers in some environments.[2] It has been demonstrated that excessive
354 concentrations of Al^{3+} and La^{3+} may be toxic to the sensitive species in waters.[2, 17]
355 *Daphnia magna* has been used to indicate eco-toxicity potential when using geo-
356 engineering materials.[44] According to previous studies, the median effect
357 concentrations (EC_{50}) of Al^{3+} and La^{3+} to *Daphnia magna* were above 3.9 and 23 mg
358 L^{-1}.[45, 46] In this study, the maximum concentrations of released Al^{3+} and La^{3+} after
359 adsorption procedure were 0.078 mg L^{-1} by LAH-1/30 and 0.077 mg L^{-1} by LAH-1/10
360 under natural water pH conditions (Figure 4), which were much lower than the reported
361 thresholds of 3.9 and 23 mg L^{-1}, respectively. Moreover, it has been reported that La^{3+}
362 and Al^{3+} ions could also bind with CO_3^{2-} and humics in aquatic environments thus
363 possibly reducing their toxicity to some extent.[47-49] Although further investigation is
364 needed under a wide range of environmental conditions, the initial findings suggest that
365 it is possible to use LAH materials at their optimal dosage for control of internal P loads
366 without causing substantial adverse effects to aquatic ecosystem.

367 **Environmental implications.** In recent decades, cost-efficient and ecologically
368 benign P locking materials have been in urgent demand in geo-engineering for
369 eutrophication control.[6, 7, 50] This study may promote the development of novel La-
370 modified materials for highly efficient P removal from water bodies. To remove one Kg

P in water bodies, the cost of LAH is 18.5 - 25.6 $/Kg P, which is less than that of Phoslock® (27.9 $/Kg P) (Table S4). The LAH composite has the potential to save up to ~ 34% cost compared to that of Phoslock®. Moreover, LAH have much higher P adsorption capacity and La use efficiency than other La-modified materials reported before (Table S5). After LAH are applied in natural waters (pH 8.5), the composition of La-hydroxide in LAH may play a primary role in locking P than Al-hydroxide (Figure 5). The combined contribution of two-component of La and Al may be an important direction to improve the P removal efficiency for the next generation of commercial products. LAH exhibited great practical potential due to its low PO_4 desorption rates and low metal ions released concentrations under natural lake pH conditions. The positively charged LAH may also have the potential in removing other negatively charged pollutants in waters, such as algal cells, arsenate and chromate. With the combination of LAH and modified local soil,[51] the toxic algae and P in waters may be removed, and the floc resuspension and P release from lake sediments can also be capped and blocked as well.[50] Considering the challenge of understanding long-term effects, further studies are needed to evaluate its impacts on aquatic ecological responses. With additional research, LAH may be a compelling candidate as a geo-engineering tool for P control.

ASSOCIATED CONTENT

Supporting Information

Details on the synthesis of $La(OH)_3$ and $Al(OH)_3$, equations used in this study and XAFS data collection and analysis. Figures showing the FESEM images of LAH, ζ potential of $La(OH)_3$ and $Al(OH)_3$, effect of pH on phosphate adsorption efficiency, phosphate desorption rates of LAH, Al/La dissolutions from LAH at varying pH 4.0-10.0, EXAFS experimental and fitted spectra, changes of solution pH and Langmuir

adsorption isotherm on mixture of $La(OH)_3$ and $Al(OH)_3$. Tables showing Langmuir isotherm parameters and phosphate specific adsorptions, EXAFS data of $La(OH)_3$, LAH and Phoslock®, cost of LAH and Phoslock® and comparison of La-modified materials. This information is available free of charge via the Internet at http://pubs.acs.org.

AUTHOR INFORMATION

Corresponding Author

*Corresponding author: Tel.: +86 10 62849686; Fax: +86 10 62849686; E-mail address: gpan@rcees.ac.cn

Notes

The authors declare no competing financial interest.

ACKNOWLEDGEMENTS

The research was supported by the Strategic Priority Research Program of CAS (XDA09030203) and National Natural Science Foundation of China (21377003). We thank the Beijing Synchrotron Radiation Facility (BSRF, China) for providing the beam time of 4B7A and 1W2B. Dr. Zheng Lei, Ma Chenyan, An Pengfei, Hu Yongfeng and Liu Wei are acknowledged for their valuable assistance with the XANES and EXAFS experiments and data analysis.

References

(1) Conley, D. J.; Paerl, H. W.; Howarth, R. W.; Boesch, D. F.; Seitzinger, S. P.; Havens, K. E.; Lancelot, C.; Likens, G. E. Controlling eutrophication: nitrogen and phosphorus. *Science* **2009,** *323* (20), 1014-1015.

(2) Douglas, G. B.; Hamilton, D. P.; Robb, M. S.; Pan, G.; Spears, B. M.; Lürling, M. Guiding principles for the development and application of solid-phase phosphorus adsorbents for freshwater ecosystems. *Aquat. Ecol.* **2016,** *50* (3), 385-405.

(3) Wang, L. J.; Pan, G.; Shi, W. Q.; Wang, Z. B.; Zhang, H. G. Manipulating nutrient limitation using modified local soils: a case study at Lake Taihu (China). *Water Res.* **2016,** *101*, 25-35.

(4) Carpenter, S. R. Eutrophication of aquatic ecosystems: bistability and soil phosphorus. *Proc. Natl. Acad. Sci. USA* **2005,** *102* (29), 10002-10005.

(5) Schindler, D. W.; Hecky, R. E.; Findlay, D. L.; Stainton, M. P.; Parker, B. R.; Paterson, M. J.; Beaty, K. G.; Lyng, M.; Kasian, S. E. Eutrophication of lakes cannot be controlled by reducing nitrogen input: results of a 37-year whole-ecosystem experiment. *Proc. Natl. Acad. Sci. USA* **2008,** *105* (32), 11254-11258.

(6) Spears, B. M.; Dudley, B.; Reitzel, K.; Rydin, E. Geo-engineering in lakes--a call for consensus. *Environ. Sci. Technol.* **2013,** *47* (9), 3953-3954.

(7) Spears, B. M.; Maberly, S. C.; Pan, G.; Mackay, E.; Bruere, A.; Corker, N.; Douglas, G.; Egemose, S.; Hamilton, D.; Hatton-Ellis, T.; Huser, B.; Li, W.; Meis, S.; Moss, B.; Lürling, M.; Phillips, G.; Yasseri, S.; Reitzel, K. Geo-engineering in lakes: a crisis of confidence? *Environ. Sci. Technol.* **2014,** *48* (17), 9977-9979.

(8) Copetti, D.; Finsterle, K.; Marziali, L.; Stefani, F.; Tartari, G.; Douglas, G.; Reitzel, K.; Spears, B. M.; Winfield, I. J.; Crosa, G.; D'Haese, P.; Yasseri, S.; Lürling, M. Eutrophication management in surface waters using lanthanum modified bentonite: A review. *Water Res.* **2016,** *97* (15), 162-174.

(9) Huang, W. Y.; Li, D.; Liu, Z. Q.; Tao, Q.; Zhu, Y.; Yang, J.; Zhang, Y. M. Kinetics, isotherm, thermodynamic, and adsorption mechanism studies of $La(OH)_3$-modified exfoliated vermiculites as highly efficient phosphate adsorbents. *Chem. Eng. J.* **2014,** *236* (2), 191-201.

(10) Huang, W. Y.; Zhu, Y.; Tang, J. P.; Yu, X.; Wang, X. L.; Li, D.; Zhang, Y. M. Lanthanum-doped ordered mesoporous hollow silica spheres as novel adsorbents for

efficient phosphate removal. *J. Mater. Chem. A* **2014,** *2* (23), 8839-8848.

(11) Dithmer, L.; Lipton, A. S.; Reitzel, K.; Warner, T. E.; Lundberg, D.; Nielsen, U. G. Characterization of phosphate sequestration by a lanthanum modified bentonite clay: a solid-state NMR, EXAFS, and PXRD study. *Environ. Sci. Technol.* **2015,** *49* (7), 4559-4566.

(12) Zhang, L.; Zhou, Q.; Liu, J. Y.; Chang, N.; Wan, L. H.; Chen, J. H. Phosphate adsorption on lanthanum hydroxide-doped activated carbon fiber. *Chem. Eng. J.* **2012,** *185-186*, 160-167.

(13) Ross, G.; Haghseresht, F.; Cloete, T. E. The effect of pH and anoxia on the performance of Phoslock®, a phosphorus binding clay. *Harmful Algae* **2008,** *7* (4), 545-550.

(14) Kumar, E.; Bhatnagar, A.; Hogland, W.; Marques, M.; Sillanpää, M. Interaction of anionic pollutants with Al-based adsorbents in aqueous media – A review. *Chem. Eng. J.* **2014,** *241* (4), 443-456.

(15) Tanada, S.; Kabayama, M.; Kawasaki, N.; Sakiyama, T.; Nakamura, T.; Araki, M.; Tamura, T. Removal of phosphate by aluminum oxide hydroxide. *J. Colloid Interf. Sci.* **2003,** *257* (1), 135-140.

(16) Lijklema, L. Interaction of orthophosphate with iron(III) and aluminum hydroxides. *Environ. Sci. Technol.* **1980,** *14* (5), 537-541.

(17) Reitzel, K.; Jensen, H. S.; Egemose, S. pH dependent dissolution of sediment aluminum in six Danish lakes treated with aluminum. *Water Res.* **2013,** *47* (3), 1409-1420.

(18) Berkowitz, J.; Anderson, M. A.; Amrhein, C. Influence of aging on phosphorus sorption to alum floc in lake water. *Water Res.* **2006,** *40* (5), 911-916.

(19) Gensemer, R. W.; Playle, R. C. The bioavailability and toxicity of aluminum in

aquatic environments. *Crit. Rev. Env. Sci. Tec.* **1999,** *29* (4), 315-450.

(20) Liu, Y. T.; Hesterberg, D. Phosphate bonding on noncrystalline Al/Fe-hydroxide coprecipitates. *Environ. Sci. Technol.* **2011,** *45* (15), 6283-6289.

(21) Khare, N.; Martin, J. D.; Hesterberg, D. Phosphate bonding configuration on ferrihydrite based on molecular orbital calculations and XANES fingerprinting. *Geochim. Cosmochim. Ac.* **2007,** *71* (18), 4405-4415.

(22) Khare, N.; Hesterberg, D.; Martin, J. D. XANES investigation of phosphate sorption in single and binary systems of iron and aluminum oxide minerals. *Environ. Sci. Technol.* **2005,** *39* (7), 2152-2160.

(23) Khare, N.; Hesterberg, D.; Beauchemin, S.; Wang, S. L. XANES determination of adsorbed phosphate distribution between ferrihydrite and boehmite in mixtures. *Soil Sci. Soc. Am. J.* **2004,** *68* (2), 460-469.

(24) Xiong, W. H.; Peng, J. Development and characterization of ferrihydrite-modified diatomite as a phosphorus adsorbent. *Water Res.* **2008,** *42* (19), 4869-4877.

(25) Zhang, M. Y.; He, G. Z.; Pan, G. Binding mechanism of arsenate on rutile (110) and (001) planes studied using grazing-incidence EXAFS measurement and DFT calculation. *Chemosphere* **2015,** *122*, 199-205.

(26) Lunsford, J. H.; Jayne, J. P. Electron paramagnetic resonance of oxygen on ZnO and ultraviolet-irradiated MgO. *J. Chem. Phys.* **1966,** *44* (4), 1487-1492.

(27) Liu, Z. E.; Cheng, J. J. EPR study on $YBa_2Cu_{3-x}M_xO_{7-\delta}$ ($M=Zn^{2+}$, Co^{3+}) oxide ceramics. *Bull. Chin. Ceramic Soc.* **1991,** *1*, 6-9.

(28) Ali, F.; Chadwicka, A. V.; Smit, M. E. EXAFS analysis of the structural evolution of gel-formed La_2O_3. *J. Mater. Chem.* **1997,** *7* (2), 285-291.

(29) Parks, G. A. The isoelectric points of solid oxides, solid hydroxides, and aqueous hydroxo complex systems. *Chem. Rev.* **1965,** *65* (2), 177-195.

(30) Wan, B.; Yan, Y. P.; Liu, F.; Tan, W. F.; He, J. J.; Feng, X. H. Surface speciation of *myo*-inositol hexakisphosphate adsorbed on TiO_2 nanoparticles and its impact on their colloidal stability in aqueous suspension: A comparative study with orthophosphate. *Sci. Total. Environ.* **2016,** *544*, 134-142.

(31) Liu, J. Y.; Zhou, Q.; Chen, J. H.; Zhang, L.; Chang, N. Phosphate adsorption on hydroxyl–iron–lanthanum doped activated carbon fiber. *Chem. Eng. J.* **2013,** *215-216*, 859-867.

(32) Rajan, S. S. S. Changes in net surface charge of hydrous alumina with phosphate adsorption. *Nature* **1976,** *262*, 45-46.

(33) Takashi, Y.; Takaki, H.; Takahiro, M.; Tsunehiro, T.; Takuzo, F. Structures and acid-base properties of La/Al_2O_3 - role of La addition to enhance thermal stability of r-Al_2O_3. *Chem. Mater.* **2003,** *15* (25), 4830-4840.

(34) Spears, B. M.; Lürling, M.; Yasseri, S.; Castro-Castellon, A. T.; Gibbs, M.; Meis, S.; McDonald, C.; McIntosh, J.; Sleep, D.; Van Oosterhout, F. Lake responses following lanthanum-modified bentonite clay (Phoslock®) application: an analysis of water column lanthanum data from 16 case study lakes. *Water Res.* **2013,** *47* (15), 5930-5942.

(35) Gerke, J. Phosphate adsorption by humic Fe-oxide mixtures aged at pH 4 and 7 and by poorly ordered Fe-oxide. *Geoderma* **1993,** *59* (1-4), 279-288.

(36) Kizewski, F. R.; Boyle, P.; Hesterberg, D.; Martin, J. D. Mixed anion (phosphate/oxalate) bonding to Iron(III) materials. *J. Am. Chem. Soc.* **2010,** *132* (7), 2301-2308.

(37) Tokarz-Sobieraj, R.; Witko, M.; Gryboś, R. Reduction and re-oxidation of molybdena and vanadia: DFT cluster model studies. *Catal. Today* **2005,** *99* (1-2), 241-253.

(38) Wu, Q. P.; Zheng, Q.; van de Krol, R. Creating oxygen vacancies as a novel

strategy to form tetrahedrally coordinated Ti^{4+} in Fe/TiO_2 nanoparticles. *J. Phys. Chem. C.* **2012,** *116* (12), 7219-7226.

(39) Perera, D. N.; Harrowell, P. Stability and structure of a supercooled liquid mixture in two dimensions. *Phys. Rev. E* **1999,** *59* (5 Pt B), 5721-5743.

(40) Brückman, K.; Grabowski, R.; Haber, J.; Mazurkiewicz, A.; Słoczyński, J.; Wiltowski, T. The role of different MoO_3 crystal faces in elementary steps of propene oxidation. *J. Catal.* **1987,** *104* (1), 71-79.

(41) Menetrey, M.; Markovits, A.; Minot, C. Reactivity of a reduced metal oxide surface hydrogen, water and carbon monoxide adsorption on oxygen defective rutile TiO_2 (110). *Surf. Sci.* **2003,** *524* (s 1-3), 49-62.

(42) Wang, J. A.; Bokhimi, X.; Morales, A.; Novaro, O.; López, T.; Gómez, R. Aluminum local environment and defects in the crystalline structure of sol-gel alumina catalyst. *J. Phys. Chem. B* **1999,** *103* (2), 299-303.

(43) Abdala, D. B.; Northrup, P. A.; Arai, Y.; Sparks, D. L. Surface loading effects on orthophosphate surface complexation at the goethite/water interface as examined by extended x-ray absorption fine structure (EXAFS) spectroscopy. *J. Colloid Interf. Sci.* **2015,** *437*, 297-303.

(44) Wang, Z. B.; Zhang, H. G.; Pan, G. Ecotoxicological assessment of flocculant modified soil for lake restoration using an integrated biotic toxicity index. *Water Res.* **2016,** *97*, 133-141.

(45) Sneller, F. E. C.; Kalf, D. F.; Weltje, L.; Van Wezel, A. P. Maximum permissible concentrations and negligible concentrations for rare earth elements (REEs). RIVM report 601501011. **2000**.

(46) Biesinge, K. E.; Christen, G. M. Effects of various metals on survival, growth, reproduction, and metabolism of *Daphnia-magna*. *J. Fish. Res. Board Can.* **1972,** *29*

546 (12), 1691-1700.
547 (47) Lee, J. H.; Byrne, R. H. Examination of comparative rare earth element
548 complexation behavior using linear free-energy relationships. *Geochim. Cosmochim.*
549 *Ac.* **1992,** *56* (3), 1127-1137.
550 (48) Dithmer, L.; Nielsen, U. G.; Lundberg, D.; Reitzel, K. Influence of dissolved
551 organic carbon on the efficiency of P sequestration by a lanthanum modified clay. *Water*
552 *Res.* **2016,** *97*, 39-46.
553 (49) Borggaard, O. K.; Raben-Lange, B.; Gimsing, A. L.; Strobel, B. W. Influence of
554 humic substances on phosphate adsorption by aluminium and iron oxides. *Geoderma*
555 **2005,** *127* (3-4), 270-279.
556 (50) Pan, G.; Dai, L. C.; Li, L.; He, L. C.; Li, H.; Bi, L.; Gulati, R. D. Reducing the
557 recruitment of sedimented algae and nutrient release into the overlying water using
558 modified soil/sand flocculation-capping in eutrophic lakes. *Environ. Sci. Technol.* **2012,**
559 *46* (9), 5077-5084.
560 (51) Pan, G.; Yang, B.; Wang, D.; Chen, H.; Tian, B. H.; Zhang, M. L.; Yuan, X. Z.;
561 Chen, J. In-lake algal bloom removal and submerged vegetation restoration using
562 modified local soils. *Ecol. Eng.* **2011,** *37* (2), 302-308.